π^0 PRODUCTION BY e^+e^- ANNIHILATION AT 14 AND 34 GeV c.m. ENERGY

TASSO Collaboration

R. BRANDELIK, W. BRAUNSCHWEIG, K. GATHER, F.J. KIRSCHFINK, K. LÜBELSMEYER, H.-U. MARTYN, G. PEISE, J. RIMKUS, H.G. SANDER, D. SCHMITZ, A. SCHULTZ von DRATZIG, D. TRINES and W. WALLRAFF
I. Physikalisches Institut der RWTH Aachen, Germany [8]

H. BOERNER, H.M. FISCHER, H. HARTMANN, E. HILGER, W. HILLEN, G. KNOP, L. KÖPKE, H. KOLANOSKI, P. LEU, R. WEDEMEYER, N. WERMES and M. WOLLSTADT
Physikalisches Institut der Universität Bonn, Germany [8]

H. BURKHARDT, S. COOPER, D. HEYLAND, H. HULTSCHIG, P. JOOS, W. KOCH, U. KÖTZ, H. KOWALSKI [1], A. LADAGE, D. LÜKE, H.L. LYNCH [2], P. MÄTTIG, K.H. MESS [3], D. NOTZ, J. PYRLIK, D.R. QUARRIE [4], R. RIETHMÜLLER, A. SHAPIRA [5], P. SÖDING, B.H. WIIK and G. WOLF
Deutsches Elektronen-Synchrotron, DESY, Hamburg, Germany

R. FOHRMANN, M. HOLDER, H.L. KRASEMANN, G. POELZ, O. RÖMER and P. SCHMÜSER
II. Institut für Experimentalphysik der Universität Hamburg, Germany [8]

I. Al-AGIL, R. BEUSELINCK, D.M. BINNIE, A.J. CAMPBELL, P.J. DORNAN, D.A. GARBUTT, T.D. JONES, W.G. JONES, S.L. LLOYD, D. PANDOULAS, J.K. SEDGBEER, R.A. STERN and S. YARKER
Department of Physics, Imperial College London, UK [9]

M.G. BOWLER, I.C. BROCK, R.J. CASHMORE, R. DEVENISH, P. GROSSMANN, J. ILLINGWORTH, M. OGG, G.L. SALMON, J. THOMAS, T.R. WYATT and C. YOUNGMAN
Department of Nuclear Physics, Oxford University, UK [9]

K.W. BELL, B. FOSTER, J.C. HART, J. PROUDFOOT, D.H. SAXON and P.L. WOODWORTH
Rutherford Appleton Laboratory, Chilton, UK [9]

E. DUCHOVNI, Y. EISENBERG, U. KARSHON, G. MIKENBERG, D. REVEL and E. RONAT
Weizmann Institute, Rehovot, Israel [10]

T. BARKLOW, J. FREEMAN [6], T. MEYER [7], G. RUDOLPH, E. WICKLUND, S.L. WU and G. ZOBERNIG
Department of Physics, University of Wisconsin, Madison, WI, USA [11]

Received 19 October 1981

The process $e^+e^- \to \pi^0$ + anything has been measured at c.m. energies of 14 and 34 GeV for π^0 energies between 0.5 and 4 GeV. The ratio of π^0 to $\pi^\pm$ production for π momenta between 0.5 and 1.5 GeV/c is measured to be $2\sigma(\pi^0)/[\sigma(\pi^+) + \sigma(\pi^-)] = 1.3 \pm 0.4$ (1.2 ± 0.4) at 14 (34) GeV. The scaled cross section $(s/\beta)\mathrm{d}\sigma/\mathrm{d}x$ when compared with lower energy (4.9–7.4 GeV) π^0 data indicates a substantial scaling violation.

[1] Now at CERN, Geneva, Switzerland.
[2] On leave at UC Santa Barbara, USA.
[3] On leave from CERN, Geneva, Switzerland.
[4] On leave from Rutherford Appleton Laboratory, UK.
[5] Minerva Fellow, on leave from Weizmann Institute, Rehovot, Israel.
[6] Now at FNAL, Batavia, USA.
[7] Now at A&M University, TX, USA.

[8] Supported by the Deutsches Bunderministerium für Forschung und Technologie.
[9] Supported by the UK Science and Engineering Research Council.
[10] Supported by the Minerva Gesellschaft für die Forschung mbH.
[11] Supported in part by the US department of Energy contract WY-76-C-02-0881.

0 031-9163/82/0000–0000/$ 02.75

We report measurements of π^0 production in

$$e^+e^- \to \pi^0 + \text{anything} \quad (1)$$

at high energies. The experiment has been performed with the TASSO detector at the e^+e^- storage ring PETRA.

A description of the detector components used for charged particle tracking can be found elsewhere [1]. Photons from π^0 decay have been detected in a liquid argon calorimeter. It consists of four mechanically separate modules mounted outside the solenoid covering polar angles θ between 42° and 138° and azimuthal angles ϕ from 30° to 150° and 210° to 330° (see fig. 1a).

Each module is subdivided into two submodules which have a common vacuum and argon tank. Both tanks have thin entrance windows made of 1.5 mm steel (vacuum tank) and of 10 mm aluminum (argon tank) corresponding to a total of 0.2 radiation lengths (RL).

Each submodule consists of a stack of 35 2 mm lead plates which are separated by 5 mm gaps filled with liquid argon (see fig. 1b). These gaps are operated as ionization chambers. The dimensions of the stack are approximately 398 X 95 X 45 cm^3 (length X width X height). The radial distance between interaction point and front face of the stack is 179 cm. The calorimeter performs three different types of measurements. It measures the energy of showering particles (in towers, see below), determines their precise location (by strips) and measures the ionization loss dE/dx of charged particles (in dE/dx gaps).

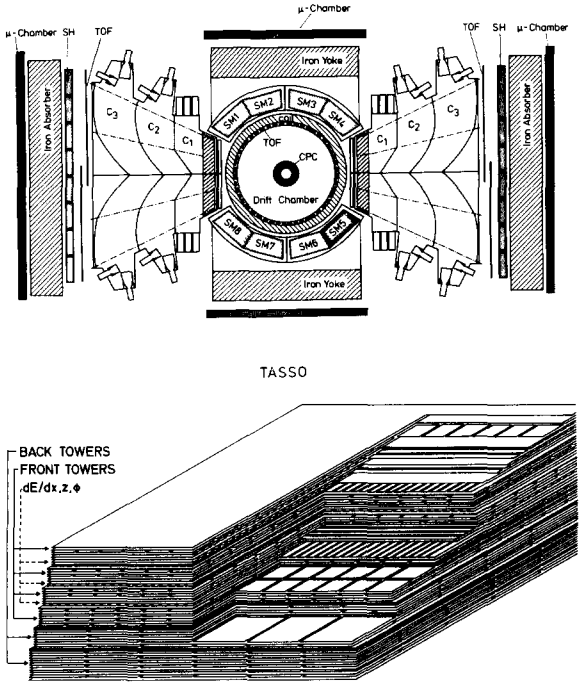

Fig. 1. (a) End view of the TASSO detector. The 8 submodules of the liquid argon calorimeter are labeled SM1, ... SM8. (b) A cut-away of a part of a liquid argon calorimeter submodule. The positions of the front towers, back towers and of the strips for dE/dx, z and ϕ measurements are marked.

For *energy* determination a technique is used that is particularly suited to the study of jets in which many particles emerge within a narrow cone. The stack is subdivided into towers directed towards the interaction point. The tower pattern is provided by the signal plates which are cut into squares of ≈7 X 7 cm^2 (front towers) and ≈14 X 14 cm^2 (back towers), respectively. Four front towers are followed by one back tower. The subdivision into front and back towers provides information on the longitudinal shower development e.g. for electron hadron discrimination. A special tower gap is mounted directly behind the entrance window to provide a first sampling of showers formed in the material in front of the stack. The total thickness of the front and back towers is 6.1 and 7.6 RL, respectively. The charge deposited on all signal plates of a given tower is collected by a single electronic channel.

A rough *position* measurement is given by the location of the front towers. For a precise measurement the stack is equipped with layers of 2 cm wide strips oriented parallel to the beam axis (ϕ = const.) and orthogonal to it (z = const.). The signal and high voltage planes of a strip layer consist of 2 mm thick epoxy printed circuit boards separated by 5 mm argon gaps. The strip layers are inserted between the tower plates. Two layers of z strips and one ϕ strip layer follow directly behind the first tower gap. Two more layers of z and ϕ strips each follow after 1.7 and 3.1 RL. The signals from corresponding strips at the same ϕ in different depths are added onto a single electronic channel. The same is true for the last two z strip layers.

The ionization loss dE/dx of charged particles is measured in the first two z strip layers.

There are in total 10 928 separate electronic channels. Each channel consists of a preamplifier, an amplifier and an analog-to-digital converter (ADC). The r.m.s.

noise level for towers is well below 10 MeV shower equivalent. The read-out threshold for towers is set to 20 MeV shower equivalent; for strips the threshold corresponds to 40% of the energy loss of a minimum ionizing particle.

The performance of each submodule has been tested at the DESY synchrotron with electron and photon beams. Without absorber material in front of the module an r.m.s. energy resolution of $\sigma/E = 0.09/\sqrt{E}$ (E in GeV) has been obtained for electrons with $E > 0.8$ GeV increasing to $\sigma/E = 0.16/\sqrt{E}$ at 0.2 GeV. In the TASSO detector the energy resolution is degraded by the material in front of the counter (beam pipe, chambers, coil etc.) which amounts to 1.6 RL including the tank walls. A detailed analysis of the energy loss in the absorber material as well as through leakage has been performed using the Monte Carlo program EGS [2] which simulated the shower development in the absorber and the calorimeter stack. Correction functions have been determined as a function of incident photon energy and angles applying the same cluster analysis as used for the data (see below). The resulting energy resolution for photons at normal incidence can be approximated by $\sigma/E = [0.11 + 0.02/(E - 0.5)]/\sqrt{E}$ for $E > 1$ GeV. The energy calibration is monitored by Bhabha scattering $e^+e^- \to e^+e^-$ detected in the calorimeter. The angular resolution for photons of energy near 1 GeV is $\sigma_\phi = 4$ mrad, $\sigma_\theta = 6$ mrad as determined by Monte Carlo studies; the measured angular resolution for high energy ($E > 10$ GeV) electrons is $\sigma_\phi \approx \sigma_\theta = 3$ mrad. The detection efficiency for photons as determined from EGS studies is 50% at 55 MeV rising to >90% above 160 MeV.

For the investigation reported in this paper multihadron events from e^+e^- annihilation have been selected in the standard way [1] using the charged particle information provided by the central detector. Charged particles with momenta transverse to the beam $p_T > 0.1$ GeV/c have been accepted for polar angles $|\cos\theta| < 0.87$. Multihadron events at a c.m. energy of $W = 14$ (34) GeV have been required to have ≥ 4 (5) accepted charged particles with a total measured momentum $\Sigma p_i > 0.27\ W$. Additional cuts [1] removed the remaining contributions from beam–gas scattering, two-photon processes and τ pair production. A total of 2173 (2797) events at $W = 14$ (34) GeV satisfying the selection criteria have been used for the analysis.

Photons have been detected by a pattern recognition program scanning the information of the calorimeter for clusters. A cluster is defined as a group of adjacent front towers with energy deposit, separated from any other clusters by front towers with shower energy below 20 MeV. The back towers associated with the front tower cluster are found and their energy is added to that measured by the front towers. Using the strip information the precise position of the cluster is determined. Taking the event vertex as the origin the θ and ϕ coordinates are computed. All charged tracks seen in the central detector are followed to see whether they can be linked to any of the clusters. Clusters for which the measured direction agrees with that predicted for a given charged track to better than 0.05 rad are called charged clusters and are ignored in the further analysis.

The remaining clusters have been assumed to originate from photons. The measured energy has been corrected for energy loss through absorption and leakage with the correction functions determined by EGS (see above). To ensure a good energy resolution a fiducial region has been defined for each submodule which required the cluster to be at least one row of front towers away from the edge of the calorimeter in ϕ and three rows of front towers in θ. The total solid angle defined by the fiducial region amounts to 36% of 4π. In order to ensure good position accuracy each cluster has been required to have at least one ϕ strip and one z strip set.

The performance of the calorimeter and of the read-out electronics has constantly been monitored using cosmic rays, Bhabha scattering ($e^+e^- \to e^+e^-$), and μ pair production ($e^+e^- \to \mu^+\mu^-$) recorded concurrently with the annihilation events. In this way any faults during data taking have been detected and the submodule in question has not been used for the corresponding running period. The efficiency of the calorimeter has been tested by selecting e^+e^- and $\mu^+\mu^-$ pairs in the central detector and searching for the corresponding clusters in the calorimeter. An efficiency of 98.8% (99.8%) has been found at 14 (34) GeV.

For each event all possible pairs of photons have been formed and their effective mass $m_{\gamma\gamma}$ and total energy $E_{\gamma\gamma}$ have been calculated. Fig. 2a shows the $m_{\gamma\gamma}$ distributions obtained at $W = 14$ and 34 GeV for $0.5 < E_{\gamma\gamma} < 4$ GeV requiring each γ to have at least $E_{\min} = 0.15$ GeV energy. A clear π^0 signal is observed.

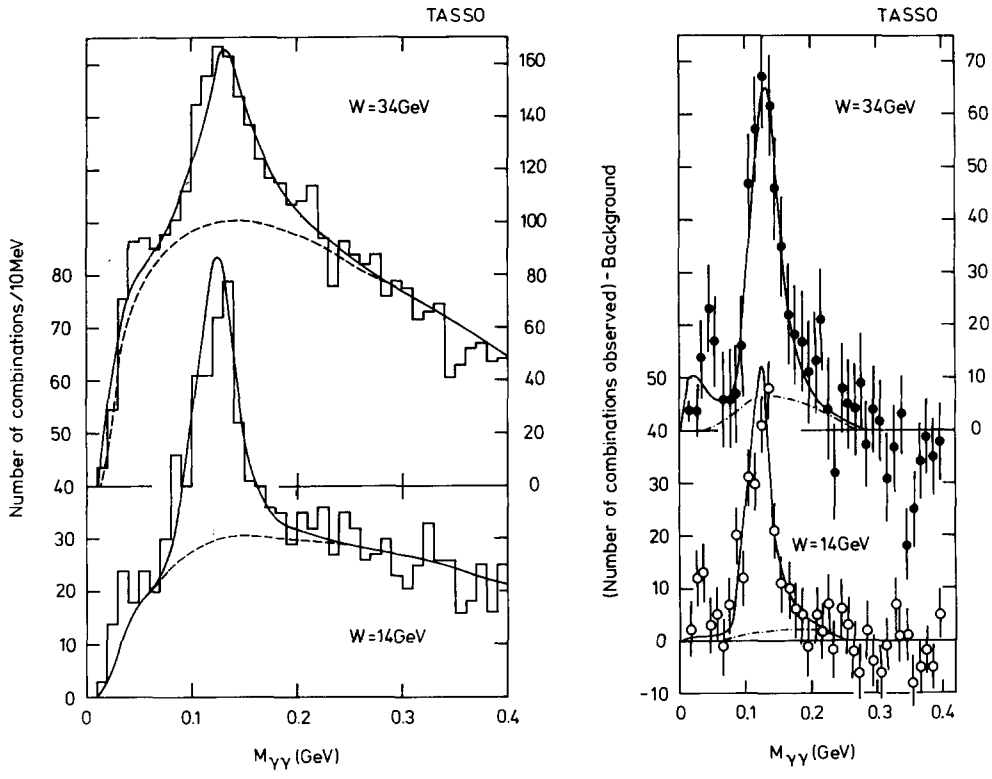

Fig. 2. (a) The $\gamma\gamma$ mass distributions measured at 14 and 34 GeV for $0.5 < E_{\gamma\gamma} < 4$ GeV and photon energies $E_\gamma > 0.15$ GeV. The dashed curves indicate the background contribution as computed from Monte Carlo (see text). The solid curves show the sum of the contributions from π^0 production and background. (b) The background-subtracted $\gamma\gamma$ mass distribution at 14 and 34 GeV for $0.5 < E_{\gamma\gamma} < 4$ GeV. The dashed–dotted curves indicate the additional background subtracted (see text). The solid curves show the π^0 signal predicted by Monte Carlo and normalized to the number of $\gamma\gamma$ combinations in the π^0 mass interval above background.

The π^0 detection efficiency as well as the shape of the background distribution in the π^0 mass region have been determined with the help of the Monte Carlo program MONSTER. The program simulates the response of the detector in full detail. Events have been generated for the process

$e^+e^- \rightarrow$ quark + antiquark + gluon

according to QCD [3] using Field–Feynman fragmentation functions [4,5] and including radiative effects [6]. Baryon production has also been included in the fragmentation [7]. This calculation was found to describe well the charged particle data [5]. All generated particles have been followed through the detector allowing for decay and secondary interactions [8] in the various materials as well as for detector inefficiencies. For charged particles the ensuing information on wire addresses, drift time, etc. has been stored. For photons and electrons the shower development has been followed with the help of EGS producing the same type of information as obtained in the experiment.

The Monte Carlo events have been passed through the analysis chain used for the real data. With these events, the loss of photons due to overlap with charged tracks or with other photons has been studied. The fraction of photons from π^0 decay which overlap with charged tracks or other photons is 10% (23%) at 14 (34) GeV.

The π^0 yield has been determined for five π^0 energy intervals, $E_{\gamma\gamma}$ = 0.5–1, 1–1.5, 1.5–2, 2–3 and 3–4 GeV. The background in the π^0 mass region has been estimated in the following way. From the accepted photons of the Monte Carlo events the $m_{\gamma\gamma}$ spectrum has been computed excluding those pairs of photons where both γ's come from the same π^0. The Monte Carlo spectrum has been normalized such that the

number of $\gamma\gamma$ combinations with $m_{\gamma\gamma} = 0.2$–0.4 GeV is the same as in the data. (The contribution from π^0 decay to this mass interval is expected to be negligible.) This has been done separately for each $E_{\gamma\gamma}$ interval. The dashed curves in fig. 2a show the prediction for the background obtained in this way. In fig. 2b the background-subtracted spectra are shown. The observed width of the π^0 signal agrees well with the expected one (see solid curves). The enhancement seen at very low masses is due mainly to cases where one of the photons from π^0 decay has produced two clusters, with one cluster carrying only a small fraction of the original photon energy. This procedure to describe the background has been found to give consistent results for $E_{\gamma\gamma} > 1$ GeV: the π^0 mass spectrum obtained by subtraction agrees well with the one predicted by the Monte Carlo calculation. In the first $E_{\gamma\gamma}$ interval (0.5–1 GeV) the subtracted spectrum has residual background which when interpolated through the π^0 mass interval amounts to 14% (36%) at 14 (34) GeV. This background contribution is shown by the dashed –dotted curves in fig. 2b. The uncertainty in this contribution is included in the error estimation of the cross sections. From the background-subtracted spectra a π^0 r.m.s. mass resolution of $\sigma_m = 0.023$ (0.031) GeV is obtained at 14 (34) GeV.

To arrive at the π^0 acceptance efficiency let N_1 be the number of Monte Carlo events generated at the nominal c.m. energy $W = W_0$ (i.e. without radiative effects) and $n_1\,(E_{\pi^0})\,\mathrm{d}E_{\pi^0}$ the number of π^0 produced in the energy range $E_{\pi^0}, E_{\pi^0} + \mathrm{d}E_{\pi^0}$; N_2 the number of Monte Carlo events generated with radiative effects and accepted by the selection criteria for hadron events; $n_2(E_{\pi^0})\,\mathrm{d}E_{\pi^0}$ the corresponding number of Monte Carlo π^0's registered by the calorimeter and reconstructed and accepted by the analysis procedure in the π^0 mass interval (0.07–0.18 GeV at 14 GeV; 0.09 –0.19 GeV at 34 GeV). The acceptance efficiency is contained in the ratio $\epsilon_{\pi^0} = (n_2/N_2)/(n_1/N_1)$. Note that ϵ_{π^0} includes not only the geometrical acceptance but also accounts for fluctuations in the shower development, for overlap of clusters, for inefficiencies of the cluster search, and for radiative effects. For those data where the information from all 8 submodules would be used ϵ_{π^0} varies between 0.05 and 0.14 for π^0 energies between 0.5 and 4 GeV. In computing ϵ_{π^0}, $n_1(E_{\pi^0})$ included *all* primary produced π^0's plus those coming from the strong, electromagnetic or weak decay of particles *except* for those from K^0 and $K^\pm$ decay. The K yields have been measured in this experiment [9,10]. Note that n_2 *includes* π^0's from K decay. (The inclusion of π^0's from K decay in n_1 would decrease ϵ_{π^0} and therefore increase the π^0 cross sections given below by a factor which is 1.16 in the first E_{π^0} interval decreasing to 1.12 in the last π^0 interval.)

The π^0 cross section has been computed from the measured number of accepted hadronic events, N_3, and the number of $\gamma\gamma$ combinations $n_3(E_{\pi^0})\,\mathrm{d}E_{\pi^0}$, observed above background in the π^0 mass interval. Denoting by σ_{tot} the total hadronic annihilation cross section the π^0 cross section is given by

$$\mathrm{d}\sigma(E_{\pi^0}) = \sigma_{\mathrm{tot}}\,\frac{1}{\epsilon_{\pi^0}}\,\frac{n_3(E_{\pi^0})\,\mathrm{d}E_{\pi^0}}{N_3}\,.$$

Figs. 3a and 3b show the differential cross section $\mathrm{d}\sigma/\mathrm{d}p$ for π^0 production and the scaled cross section $(s/\beta)\,\mathrm{d}\sigma/\mathrm{d}x$ ($s = W^2$, $\beta = p/E$ and $x = 2E/W$ where p, E are the π^0 momentum and energy) for $W = 14$ and 34 GeV. The error bars include the statistical error as well as the uncertainties in background subtraction (typically of the order of 10%), acceptance (≈8%), efficiency of the calorimeter (5%) and cross section normalization (8%) which have been added in quadrature.

Fig. 3b also exhibits the averages of the π^+ and π^- cross section $0.5\,[\sigma(\pi^+) + \sigma(\pi^-)]$ measured previously at $W = 12$ and 30 GeV by this experiment [10]. They agree well with the π^0 cross sections. By scaling these charged pion cross sections to $W = 14$ (34) GeV assuming a W dependence $\sigma \sim W^{-2}$ we find for the pion energy interval $0.5 < E_\pi < 1.5$ GeV for which both π^0 and $\pi^\pm$ data are available:

$$\frac{2\sigma(\pi^0)}{\sigma(\pi^+) + \sigma(\pi^-)} = 1.3 \pm 0.4 \quad (1.2 \pm 0.4)$$

at 14 (34) GeV. This result is consistent with equal yields of π^0, π^+ and π^-.

Fig. 3b shows that the scaled π^0 cross sections for W at 14 and 34 GeV agree within errors in the x direction where both sets overlap ($x = 0.1$–0.2). However, the comparison of our data with those measured [11] at lower energy (4.9–7.4 GeV) suggests a sizeable scaling violation (see fig. 3b): for x between 0.2 and 0.6 the low energy data are roughly a factor of 2 above

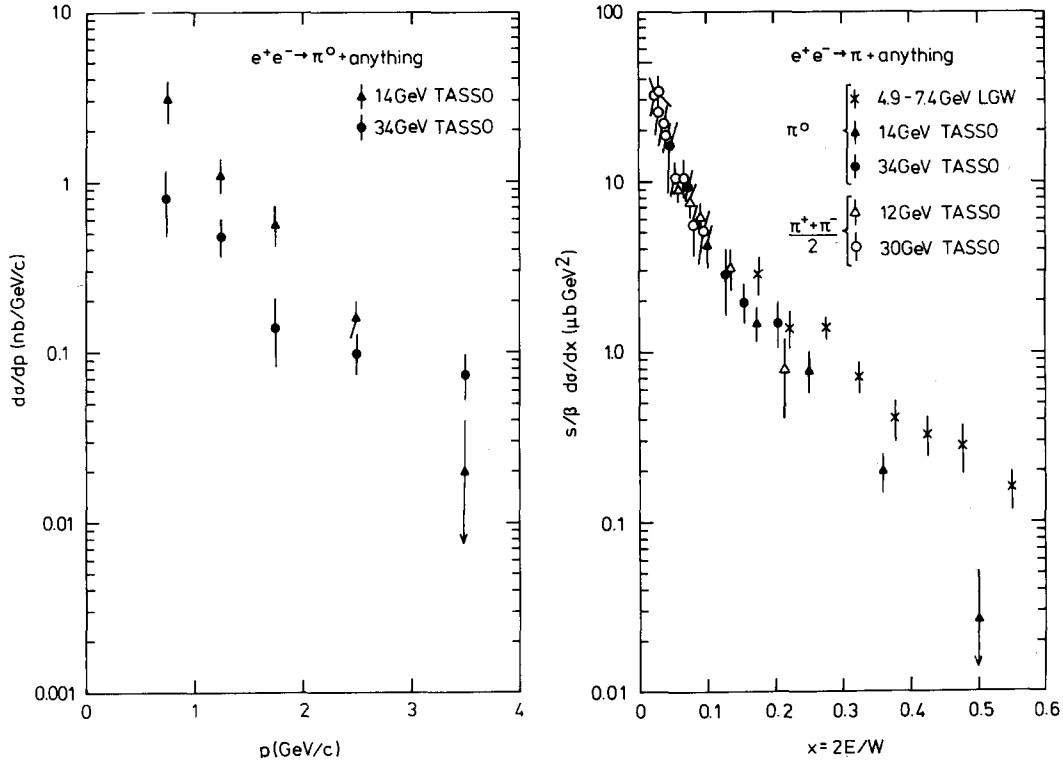

Fig. 3. (a) The differential cross section $d\sigma/dp$ for $e^+e^- \to \pi^0$ + anything at W = 14 and 34 GeV. π^0's from K decay are excluded. (b) The scaled cross section $(s/\beta)\, d\sigma/dx$ for $e^+e^- \to \pi^0$ + anything at W = 14 and 34 GeV (π^0's from K decay excluded), and at 4.9–7.4 GeV by ref. [11]. Also shown are the averages of π^+ and π^- production, 0.5 $[\sigma(\pi^+) + \sigma(\pi^-)]$, as measured at 12 and 30 GeV [10].

those from 14 GeV. The scaling violations cannot be a result of the bottom threshold which is crossed between the low and high energy data since bottom quark production could only raise the π^0 cross section at higher W energies.

The design, construction and installation of the liquid argon calorimeters required the effort of many people. We thank the DESY directorate, in particular Professors E. Lohrmann, H. Schopper, G.-A. Voss, G. Weber, and also Dr. G. Söhngen for their continuous support. We are deeply indebted to Mr. A. Papakonstantinou and Mr. M. Müller for design and supervision of the construction of the tanks. In the construction of the stacks, the electronics and the programs for read-in and testing Messrs. M. Boehnert, D. Hoppe, A. Jacob, M. Klinkmüller, G. Kraft, W. Neff, P. Rattke, K. Rehlich, H.-H. Sabath, W. Schütte, K. Sperber, K. Westphal, K.-H. Wroblewski and Mrs. H. Siegner have done a superb job. We are also indebted to Mr. F. Czempik and Dr. F. Schwickert for their invaluable help with the installation. We are grateful to Dr. R. Nelson for help with EGS.

[1] TASSO Collab., R. Brandelik et al., Z. Phys. C4 (1980) 87; Phys. Lett. 83B (1979) 621.
[2] R.L. Ford and W.R. Nelson, SLAC Report 210 (1978).
[3] P. Hoyer et al., Nucl. Phys. B161 (1979) 349.
[4] R.D. Field and R.P. Feynman, Nucl. Phys. B136 (1978) 1.
[5] TASSO Collab., R. Brandelik et al., Phys. Lett. 94B (1980) 437.
[6] F.A. Berends and R. Kleiss, DESY Reports 80/66 (1980) and 80/73 (1980).
[7] T. Meyer, DESY Report 81/46 (1981).
[8] A. Grant, Nucl. Instrum. Methods 131 (1975) 167.
[9] TASSO Collab., R. Brandelik et al., Phys. Lett. 94B (1980) 91; 105B (1981) 75.
[10] TASSO Collab., R. Brandelik et al., Phys. Lett. 94B (1980) 444.
[11] D.L. Scharre et al., Phys. Rev. Lett. 41 (1978) 1005.